Physica Scripta

PAPER

Rotating disk: new physics discovered alongside the Sagnac effect

Mathieu Rouaud
Independent Researcher, Boudiguen 29310 Querrien, France
E-mail: mathieu137@gmail.com

Keywords: rotating disk, special relativity, Sagnac effect, Coriolis, transition, gyrometer, atom laser

OPEN ACCESS

RECEIVED
17 May 2023

REVISED
16 November 2023

ACCEPTED FOR PUBLICATION
4 December 2023

PUBLISHED
25 January 2024

Abstract

The description of the rotating disk in special relativity is revisited to find a new property that could help to improve the performance of gyrometers. On a rotating disk, two particles which bounce in opposite directions at the vertices of a regular polygon are considered. On the return to the entry point, a clock measures the time difference. A particle moving in the direction of the rotation of the disc needs more time to make one complete turn. Even if that particle is a photon, as in the original Sagnac experiment. In this paper, the time difference is explained by the difference between clockwise and counter-clockwise trajectories, due to different Coriolis effects. The particular case of the slow disk where the two trajectories are very close and almost polygonal is studied. The theoretical existence of a transition between a classical and a relativistic regime is proved, and an experimental verification with an atomic interferometer is proposed. Although the novel effect discovered and the well-known Sagnac effect seem analogous, in detail, their behavior is quite different.

1. Introduction

The roundtrip time nonreciprocity is studied for matter particles as well as for light. This effect was experimentally verified, for the first time, with light, by Georges Sagnac in 1913 [1], but afterwards, also with all kinds of particles like neutrons [2, 3], electrons [4] or atoms [5–7]. The time difference measured for the opposite roundtrip directions in a rotating closed-path is called $\Delta\tau$. The effect is present in a closed path of any shape. In the case of the historical Sagnac effect, $\Delta\tau$ is independent of the particle speed v [8–11].

In this paper, a novel effect is theoretically shown, which differs from the Sagnac effect in two ways: firstly, this new effect is absent in the case of a circular trajectory, and secondly, it varies with the particle speed v. This novel effect seems within reach of today's atom gyrometers. As shown in section 5, the experiments carried out in 1997 by Lenef *et al* [6] and Gustavson *et al* [7] were already close.

The classical study, with the example of a child on a merry-go-round with a ball, allows to grasp one of the origins of the effect. The Coriolis force explains the difference in trajectory depending on the particle's direction, however the system studied here is very different from Coriolis force gyroscopes [12].

For a rigorous study, paths in the shape of n-sided regular polygons are considered figure 1. A circular contour is not directly envisaged because it is not experimentally feasible with particles or light rays. A free particle does not follow a circular path. The circle can be approached but the approximation is not obvious and contains ambiguities. Moreover, the original experiment of Georges Sagnac was carried out according to a polygonal contour, and some of today's gyrolasers, used daily in aeronautics for navigation, are made of a polygonal laser cavity. It can be shown that the trajectory in the direction of rotation is not the same as the one in the opposite direction, both for light and matter, which explains the roundtrip time difference. It is interesting to note that even today, the Sagnac effect remains open to debate as to its theoretical interpretation in the context of special relativity [13–16].

The paper is organized as follows: in section 2, the time difference $\Delta\tau$ is calculated using classical mechanics. In section 3, the calculation uses special relativity. The Sagnac effect is found again, but alongside the novel effect added in equation (11). In section 4, the transition between the two effects is described. In section 5, an experiment with an atom gyrometer is presented. Section 6 gives the conclusion.

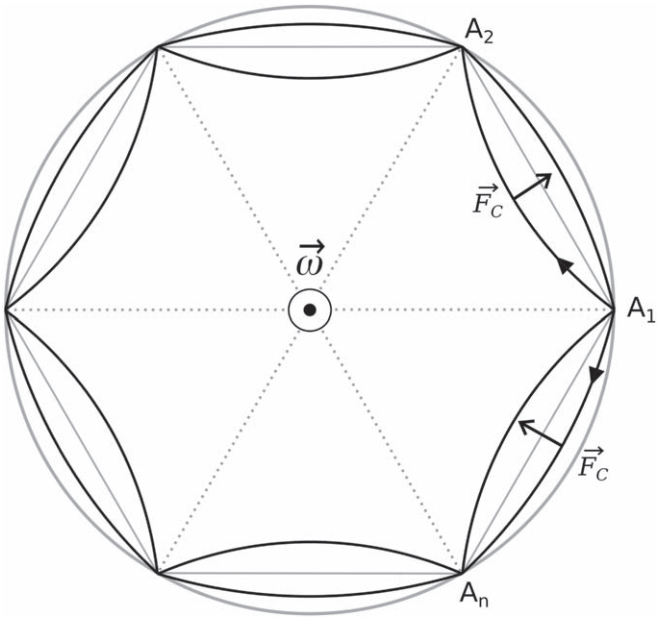

Figure 1. On a rotating disk of angular speed ω, two particles bounce in opposite directions at the vertices A_i of a regular polygon ($i \in [\![2; n]\!]$). A_1 is both the entry and the return point where the time difference is measured. Due to the Coriolis effect, the trajectories are different in the clockwise and counterclockwise directions. For the classical study, the Coriolis force $\vec{F}_C$ is considered.

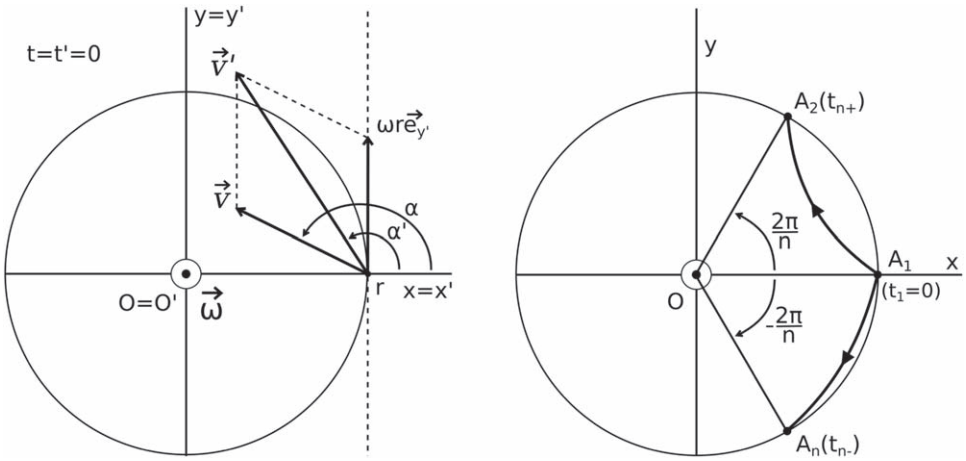

Figure 2. Velocities angles with respect to the abscissa axis : $\alpha,\ \alpha' \in]\frac{\pi}{2}, \frac{3\pi}{2}[$. Time to reach two adjacent vertexes : $t_{n\pm}$. Duration of a turn : $t_\pm = nt_{n\pm}$. Time difference: $\Delta t = t_+ - t_-$.

2. Classical novel effect

As is appropriate, light will be studied later in the relativistic framework.

2.1. Trajectories and time difference

In the inertial reference frame R' of the laboratory, where the disk is rotating with the angular frequency ω, a Cartesian system of coordinates $(O',\ x',\ y',\ z')$ is considered. At the instant $t' = 0$, the particle is at the position $A_1 = (r, 0, 0)$ with an initial velocity $\vec{v}'$ orthogonal to the rotation axis $(O'z')$. On figure 2, the quantities are defined.

For a free particle, the trajectory is rectilinear:

$$x' = v' \cos \alpha' t' + r, \quad y' = v' \sin \alpha' t' \quad \text{and} \quad z' = 0 \tag{1}$$

The non-inertial reference frame of the disk is denoted by R with the coordinates (O, x, y, z). The center of the disk is $O = O'$, and at the date $t = 0$, $(O,\ x) = (O',\ x')$. The following change of polar coordinates for a counterclockwise rotating disk is used:

$$\rho = \rho', \quad \theta = \theta' - \omega t', \quad z = z' \quad \text{and} \quad t = t' \tag{2}$$

On the disk, from A_1, at $t = 0$ the particle is thrown with the speed v and the direction α. The additivity of velocities give the initial quantities v' and α' in R':

$$\vec{v}\,' = \vec{v} + \vec{v}_{A_1/R'} \quad \Rightarrow \quad v'\cos\alpha' = v\cos\alpha, \quad v'\sin\alpha' = v\sin\alpha + \omega r$$
$$\text{and} \quad v' = v\sqrt{\cos^2\alpha + \left(\sin\alpha + \frac{\omega r}{v}\right)^2}, \quad \alpha' = \arctan\left(\frac{\sin\alpha + \frac{\omega r}{v}}{\cos\alpha}\right) + \pi \tag{3}$$

Then, for $t \in [0, t_n]$, the trajectory on the disk frame is obtained:

$$\rho = \sqrt{(v\cos\alpha t + r)^2 + (v\sin\alpha + \omega r)^2 t^2}$$
$$\text{and} \quad \theta = \arctan\left(\frac{(v\sin\alpha + \omega r)t}{v\cos\alpha t + r}\right) - \omega t + k\pi, \quad k \in \mathbb{Z} \tag{4}$$

On figure 1, with equation (4), the difference of trajectories is shown for $r = 2$ m, a period $T = 120$ s, an initial speed $v = 0.3$ m/s, and $n = 6$. The time difference found numerically is $\Delta t \simeq 1.1$ s. For $n = 4$, it is even more: $\Delta t \simeq 1.9$ s. A child with a ball on a merry-go-round can easily measure the classical time difference.

2.2. Slow disk

The disk is slow compared to the speed of the particles. If the particle speed v' is large compared to the disk speed ωr the trajectories are close to a succession of straight lines. $\rho(t_{n\pm}) = r$ and $\theta(t_{n\pm}) = \pm 2\pi/n$, then a series expansion is performed on ωt_n, and an analytical expression of $t_{n\pm}$ is obtained (Appendix A):

$$t_{n\pm} \simeq \frac{2r\sin\frac{\pi}{n}}{v} + \frac{r\sin\frac{\pi}{n}}{2v}\omega^2 t_n^2 \pm \frac{r\cos\frac{\pi}{n}}{3v}\omega^3 t_n^3 \tag{5}$$

and $\Delta t = n(t_{n+} - t_{n-})$, the classical novel effect:

$$\Delta t \simeq \frac{16}{3}\frac{\omega^3 r^4}{v^4} n\cos\frac{\pi}{n}\sin^3\frac{\pi}{n} \tag{6}$$

The term of order zero of the $t = nt_n$ expansion is L_n/v, where $L_n = 2nr\sin(\pi/n)$ is the perimeter of the polygon. There is no first-order terms The second-order term is the same for counterclockwise and clockwise particles. So, only the third order term contributes to the time difference Δt. Equation (6) shows the classical novel effect proposed in this paper. At the circle limit, when n tends to infinite, the classical time difference tends to zero. Also, this novel effect varies with v.

A first-order term would have been proportional to ωA_n, where $A_n = nr^2\sin(\pi/n)\cos(\pi/n)$ is the polygon area. As discussed later, this is the case for the relativistic Sagnac effect, for which the circle limit is non-null and there is no dependence on v. Thus, although at a first sight the classical and relativistic effects are analogs, in the details theirs natures are quite different.

3. Relativistic Sagnac and novel effects

3.1. Trajectories and time difference

The clocks in the inertial frame R' are synchronized with Einstein's synchronization method [17, 18]. In the non-inertial disk reference frame R, the proper clocks cannot be synchronized. The reference frame of the disk is *stationary* and *coordinate clocks* [9] are used. O's clock is the master clock used to synchronize all the coordinate clocks, so we have $t = t'$.

On the disk, from A_1, at $t = 0$ the particle is thrown with the speed v and the direction α. The law of composition of velocities gives a relation between the velocities measured by two inertial observers. One observer is at rest in R', but the second observer cannot be the one at rest on the disk, because the disk frame is not inertial. So the inertial reference frame coinciding locally at A_1 and $t = 0$ is chosen, because, according to the *equivalence principle*, for any space-time event there is, locally, a coinciding inertial reference frame. This local Minkowskian observer, and the neighboring observers, use their standard rulers and proper clocks to measure the local velocity: $v_{loc} = dl/dt_{loc}$ with $dt_{loc} = d\tau$. Whereas the non-inertial observer coinciding at rest on the disk, uses his coordinate clock and obtains the coordinate velocity: $v = v_{coord} = dl/dt_{coord}$, $dt_{coord} = dt = \gamma_D d\tau$ and $v_{loc} = \gamma_D v$ with $\beta_D = \omega r/c$ and $\gamma_D = 1/\sqrt{1 - \beta_D^2}$ according to the metric in the rotating disk [17]. Considering all of the above, the composition of velocities gives the initial quantities v' and α' in R':

$$\vec{v'} = \left(\frac{(v_x)_{loc}}{\gamma_D(1 + \beta_D(v_y)_{loc}/c)}, \frac{(v_y)_{loc} + \omega r}{1 + \beta_D(v_y)_{loc}/c} \right)$$
$$= \left(\frac{v\cos\alpha}{1 + \beta_D\gamma_D v\sin\alpha/c}, \frac{\gamma_D v\sin\alpha + c\beta_D}{1 + \beta_D\gamma_D v\sin\alpha/c} \right) = (v'\cos\alpha\,', v'\sin\alpha\,')$$
$$\text{and} \quad v' = v\frac{\sqrt{\cos^2\alpha + \left(\gamma_D\sin\alpha + \frac{\omega r}{v}\right)^2}}{1 + \beta_D\gamma_D v\sin\alpha/c}, \quad \alpha' = \arctan\left(\frac{\gamma_D\sin\alpha + \frac{\omega r}{v}}{\cos\alpha}\right) + \pi \tag{7}$$

Then, for $t \in [0, t_n]$, the trajectory on the disk frame is obtained:

$$\rho = \frac{\sqrt{[v\cos\alpha t + r(1 + \beta_D\gamma_D v\sin\alpha/c)]^2 + (\gamma_D v\sin\alpha + c\beta_D)^2 t^2}}{1 + \beta_D\gamma_D v\sin\alpha/c}$$
$$\text{and} \quad \theta = \arctan\left(\frac{(\gamma_D v\sin\alpha + c\beta_D)t}{v\cos\alpha t + r(1 + \beta_D\gamma_D v\sin\alpha/c)}\right) - \omega t + k\pi, \quad k \in \mathbb{Z} \tag{8}$$

The trajectories for all particles and all rotation speeds can be determined.

3.2. Slow disk

If the particle speed v' is large compared to the disk speed ωr the trajectories are close to a succession of straight lines. $\rho(t_{n\pm}) = r$ and $\theta(t_{n\pm}) = \pm 2\pi/n$, an a series expansion on $\epsilon = \omega r/v$ is performed. Indeed $v \simeq v'$ and $\epsilon << 1$. An analytical expression of Δt with $\beta_c = v/c$ is obtained (Appendix B):

$$\begin{aligned}\omega t_{n\pm} = {} & 2\epsilon\sin\frac{\pi}{n} \pm 2\epsilon^2\beta_c{}^2\sin\frac{\pi}{n}\cos\frac{\pi}{n} \\ & + \epsilon^3\sin\frac{\pi}{n}\left[2\sin^2\frac{\pi}{n} + \beta_c{}^2\left(1 - 5\sin^2\frac{\pi}{n}\right)\right] \\ & \pm 2\epsilon^4\sin\frac{\pi}{n}\cos\frac{\pi}{n}\left[\frac{4}{3}\sin^2\frac{\pi}{n} - 2\beta_c{}^2\sin^2\frac{\pi}{n} + \beta_c{}^4\left(1 - 2\sin^2\frac{\pi}{n}\right)\right] \\ & + o(\epsilon^5)\end{aligned} \tag{9}$$

Coordinate time difference for the slow disk:

$$\Delta t \simeq 4\frac{\omega A_n}{c^2} + 4\frac{\omega^3 r^2}{v^4}A_n\left[\frac{4}{3}\sin^2\frac{\pi}{n} - 2\beta_c{}^2\sin^2\frac{\pi}{n} + \beta_c{}^4\left(1 - 2\sin^2\frac{\pi}{n}\right)\right] \tag{10}$$

Proper time difference with $\Delta\tau = \Delta t/\gamma_D$ and $\gamma_D = 1/\sqrt{1 - \epsilon^2\beta_c{}^2}$:

$$\begin{aligned}\Delta\tau \simeq {} & \underbrace{4\frac{\omega A_n}{c^2}\left[1 + \frac{\omega^2 r^2}{c^2}\left(\frac{1}{2} - \frac{1}{3}\sin^2\frac{\pi}{n}\right)\right]}_{\text{Sagnac effect}} \\ & \underbrace{+ 4\frac{\omega^3 r^2}{v^4}A_n\left[\frac{4}{3}\sin^2\frac{\pi}{n} - 2\beta_c{}^2\sin^2\frac{\pi}{n} - \frac{5}{3}\beta_c{}^4\sin^2\frac{\pi}{n}\right]}_{\text{novel effect}}\end{aligned} \tag{11}$$

This formula works for all particles. Whether light or matter.

In the first part of equation (11), the genuine Sagnac effect terms are placed. The second-order term in ϵ, $\Delta\tau = 4\omega A/c^2$, is the main Sagnac effect. At fourth-order, corrections due to time dilation are added: the contour is not circular, so the full well-known Sagnac effect is obtained by integrating explicitly on the polygonal contour using the formula [19, 20] $\Delta\tau = \oint 4w\gamma_D\,\mathrm{d}A/c^2$.

The novel effect appears in the second part of equation (11), from three new terms First, the purely classical term is found again (see equation (6)). Although this term is at a higher order, it dominates when the particle speed v becomes sufficiently low (see the next section 4). The other two new terms discovered are of relativistic origin. The third term is independent of the speed v of the particle, and therefore obeys the same criterion of *universality* as the Sagnac effect.

At the fourth-order, even for the luminous Sagnac effect, obtained with $v \simeq v_{loc} = c$, a novel effect is added. However, in the limit case of the circle, when n tends to infinity, there is no novel effect for both light and matter.

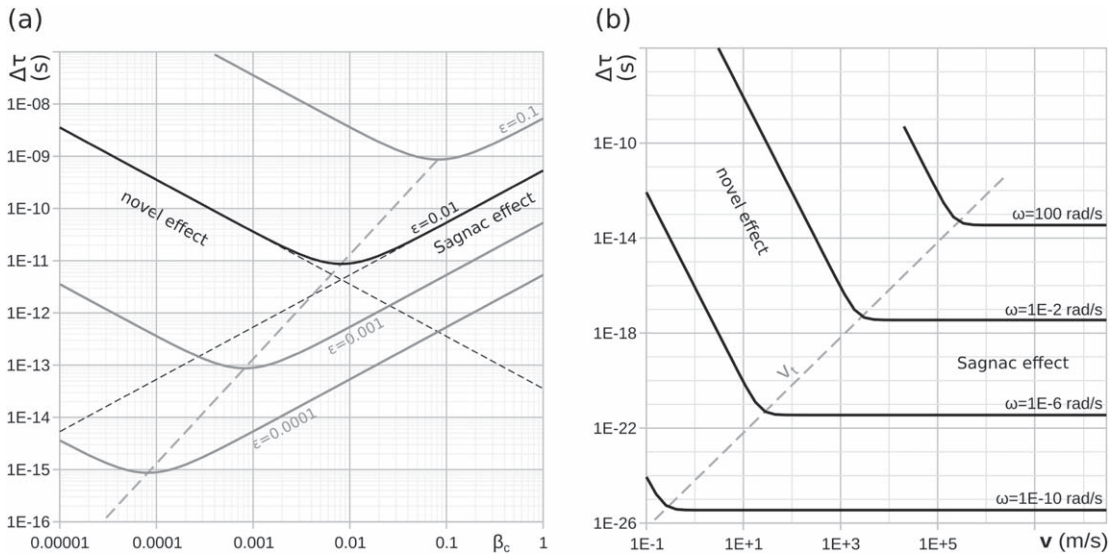

Figure 3. Time difference, transition from classical to relativistic. $\Delta\tau$ as a function of the particles speed. Figures for $r = 2$ m and $n = 4$. (a) Slow disk with $\omega r/v = \epsilon = const$. Before the transition, when $v << v_t$, $\Delta\tau \propto 1/\beta_c$, and after $\Delta\tau \propto \beta_c$. (b) Curves with $\omega = const$ and $\epsilon < 0.01$. Before the transition $\Delta\tau \propto 1/v^4$ and after $\Delta\tau = const$.

4. Results and discussions

In the limit of the slow disk, in formula 11, appears the classical regime ($c \to +\infty$), the relativistic regime ($v_{loc} \to c$) and the transition between the two. On figure 3(a), for each curve the ratio ϵ, between the disk speed ωr on the rim and the initial particle coordinate speed v on the disk, is kept constant. In the classical regime the Sagnac effect is inversely proportional to β_c, whereas in the relativistic regime the Sagnac effect is proportional to β_c. At the transition, a minimal value of $\Delta\tau$ for $\beta_{c\,\min} = 2/\sqrt{3}\ \epsilon\ \sin(\pi/n)$ is obtained. From a practical point of view, it is interesting to plot the curves for fixed rotation rates. On figure 3(b), the transition appears at the critical speed v_t defined at the crossover when the two terms in equation (11) are equal :

$$v_t = \sqrt[4]{\frac{4}{3}\omega^2 r^2 c^2 \sin^2\frac{\pi}{n}} \tag{12}$$

For a circular path, there is no transition, and the behavior is always relativistic. In the relativistic regime the Sagnac effect is independent of the speed v of the particle. It works for a light ray in a medium or a particle of matter. This is the so called *universality of the Sagnac effect* [13].

5. Proposal for an atom gyrometer experiment

With the current progress of atomic interferometers, an experiment can be proposed. In the Sagnac experiment, instead of looking at the difference in time when the rays return, the wave aspect of light is considered, and the phase shift $\Delta\phi$ is measured. Nowadays, the same is done with atoms that follow two different paths and then interfere in a Mach–Zehnder-type interferometer [21–23] figure 4. The inherent sensitivity of atom gyrometers exceeds that of photon gyrometers by several orders of magnitude [7, 24].

Let us now consider a symmetrical interferometer [25]. The paths are diamond-shaped, and the laser light pulses are considered to act as splitters and mirrors (figure 4 (b)). The calculations of subsection 3.2 are resumed with $\rho(t_A = 0) = r_M$, $\rho(t_{B_\pm}) = r_m$ and $\theta(t_{B_\pm}) = \pm\pi/2$. A series expansion on $\epsilon = \omega r_M/v$ is performed. Considering symmetries $\Delta t_{AB} = \Delta t_{BC}$, then:

$$\Delta t \simeq 2\frac{\omega A}{c^2} + \frac{2}{3}\frac{\omega^3 l^2 A}{v^4}\left(1 - \frac{3}{2}{\beta_c}^2\right) \quad \text{with} \quad l = \sqrt{r_M^2 + r_m^2} \tag{13}$$

In the context of the experiments carried out, $v << c$, $\beta_D << 1$ and $\Delta\tau \simeq \Delta t$, so:

$$\Delta\tau \simeq 2\frac{\omega A}{c^2} + \frac{2}{3}\frac{\omega^3 l^2 A}{v^4} \tag{14}$$

This result is for a half roundtrip as opposed to $\Delta\tau$ in equation (11) where a complete roundtrip is considered. Using the result of J Anandan [26], $\Delta\phi/\pi = (2mc^2/h)\Delta\tau$, then:

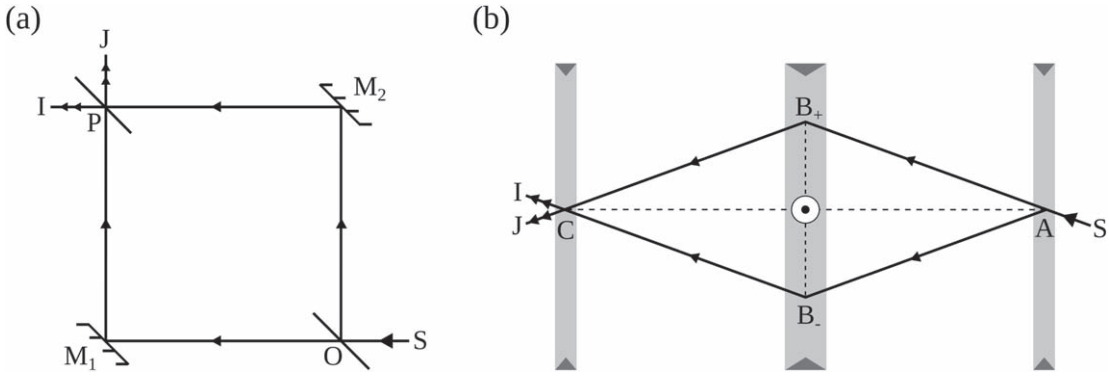

Figure 4. (**a**) Mach–Zehnder interferometer: a coherent light source S, such as a laser, emits a light ray which encounter at O a first half-silvered mirror, so half of the light is transmitted to the mirror M_1, while the other half is reflected by M_2. Both beams recombine at P with the second beam splitter and interfere on the detector I. Due to front-surface reflections the interference is destructive at J. Unlike a Sagnac interferometer, here the entry and return points are different, and the particles interfere after only a half roundtrip. (**b**) Atom interferometer: compared to the traditional optical interferometer (a), light and matter invert their roles. A coherent atomic beam S is split by a laser into two beams, which after a certain distance are redirected to each other with another laser.

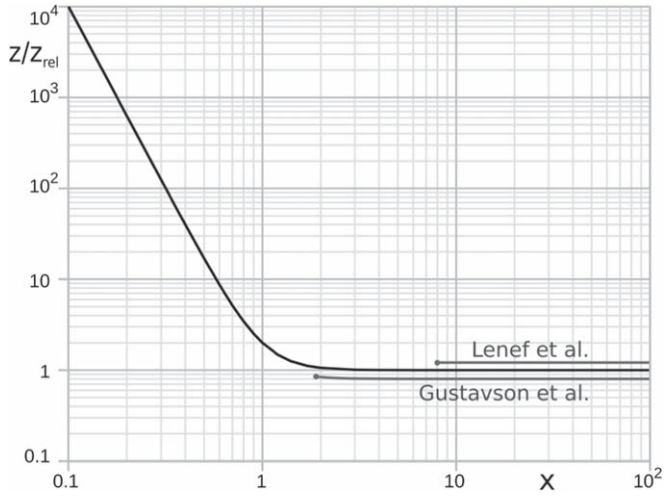

Figure 5. Two experiments results represented on the dimensionless curve z/z_{rel} versus $x = v/v_t$ with $v_t = \sqrt[4]{\omega^2 l^2 c^2/3}$. The fringe shift compared with the relativistic limit: $z/z_{rel} = 1 + 1/x^4$ with $z_{rel} = 4m\omega A/h$.

$$z = \frac{\Delta\phi}{\pi} \simeq \frac{4m\omega A}{h}\left(1 + \frac{c^2\omega^2 l^2}{3v^4}\right) \tag{15}$$

On figure 5, two curves are plotted and the results of the Lenef *et al* [6] and Gustavson *et al* [7] experiments are compared. The angular rates ω are of the order of the Earth's rotation rate and a phase shift of several fringes is obtained. The Lenef *et al* experiment use a beam of *Na* atoms with $v \simeq 1030$ m/s, $r_M \simeq 0.66$ m, $r_m \simeq 27,8$ μm, $A \simeq 37$ mm^2, and ω ranges up to 146 μrad/s. The Gustavson *et al* experiment use a beam of *Cs* atoms with $v \simeq 290$ m/s, $r_M \simeq 0.96$ m, $r_m \simeq 11.5$ μm, $A \simeq 22$ mm^2, and ω ranges up to 145 μrad/s. The maximum relative correction arising from the second term of equation (14) is 0.025% for the Lenef *et al* experiment, and 8.2% for the Gustavson *et al* experiment. In this last experiment the transition is approached.

6. Conclusion

In the particular case of an n-sided polygon, and of a slow disk compared to particle velocities, the existence of a new effect in addition to the well-known Sagnac effect is shown. This correction has been obtained by taking into account the difference between the trajectories of particles moving counterclockwise and clockwise. This novel effect is even dominant below a critical particle speed v_t. It would be very interesting to conduct experiments to study this transition. The more is known about the theoretical aspects of the roundtrip time nonreciprocity on a rotating disk, the better the accuracy of future gyrometers can be.

Data availability statement

No new data were created or analysed in this study.

Appendix A. Classical

To demonstrate equation (6), a series expansion on $x = nt_n/T$ is performed. Indeed, for a slow disk $v' >> \omega r$ and $v \simeq v'$, so $T >> nt_n$ and $x << 1$. As well as for $\omega t_n = 2\pi t_n/T = (2\pi/n)x << 1$. The coordinates $\rho(t_{n\pm}) = r$ and $\theta(t_{n\pm}) = \pm 2\pi/n$ of the first vertex reached are set in equation (4), then:

$$\begin{cases} r^2 = (v\cos\alpha_n t_n + r)^2 + (v\sin\alpha_n + \omega r)^2 t_n^2 \\ \tan\theta_n' = \dfrac{y_n'}{x_n'} \quad \Rightarrow \quad \tan(\pm 2\pi/n + \omega t_n) = \dfrac{(v\sin\alpha_n + \omega r)t_n}{v\cos\alpha_n t_n + r} \end{cases}$$

With $\theta_n' = \pm 2\pi/n + \omega t_n$, and where α_n is the value of α to obtain a n-sided regular polygon. In these equations, there are two unknown parameters, α_n and t_n. α_n is eliminated in order to provide an analytical expression of $\Delta t = n(t_{n+} - t_{n-})$:

$$\begin{cases} \dfrac{v\cos\alpha_n t_n}{r} = \dfrac{1}{\sqrt{1+\tan^2\theta_n'}} - 1 \quad \text{if} \quad n > 4 \quad \text{then} \quad x_n' \geqslant 0 \\ \dfrac{v\sin\alpha_n t_n}{r} = \pm\dfrac{1}{\sqrt{1+1/\tan^2\theta_n'}} - \omega t_n \quad \text{if} \quad \text{clockwise} \quad y_n' \geqslant 0 \quad \text{else} \quad y_n' < 0 \end{cases}$$

$$\text{then} \quad \frac{vt_n}{r} = \sqrt{\left(\frac{1}{\sqrt{1+\tan^2\theta_n'}} - 1\right)^2 + \left(\pm\frac{1}{\sqrt{1+1/\tan^2\theta_n'}} - \omega t_n\right)^2}$$

The quantities are expressed with the infinitesimal x:

$$\frac{1}{\sqrt{1+\tan^2\theta_n'}} = |\cos\theta_n'| = \cos\left(\frac{2\pi}{n}(1\pm x)\right), \quad \text{with} \quad x_n' \geqslant 0,$$
$$\text{and} \quad \frac{1}{\sqrt{1+1/\tan^2\theta_n'}} = |\sin\theta_n'| = \sin\left(\frac{2\pi}{n}(1\pm x)\right)$$

If $x_n' < 0$ the signs balance out and the same expression is obtained. The expression is then ready to be expanded:

$$\frac{vt_n}{r} = \sqrt{\left(\cos\left(\frac{2\pi}{n}(1\pm x)\right) - 1\right)^2 + \left(\pm\sin\left(\frac{2\pi}{n}(1\pm x)\right) - \omega t_n\right)^2}$$
$$= \sqrt{2 - 2\cos\left(\frac{2\pi}{n}(1\pm x)\right) \mp 2\sin\left(\frac{2\pi}{n}(1\pm x)\right)\frac{2\pi}{n}x + \left(\frac{2\pi}{n}\right)^2 x^2}$$

Series expansion on x:

$$\underbrace{\frac{vt_n}{r}}_{\text{order 0}} = \underbrace{2\sin\left(\frac{\pi}{n}\right)}_{\text{order 0}} + \underbrace{2\sin\left(\frac{\pi}{n}\right)\left(\frac{\pi x}{n}\right)^2}_{\text{order 2}} \pm \underbrace{\frac{8}{3}\cos\left(\frac{\pi}{n}\right)\left(\frac{\pi x}{n}\right)^3}_{\text{order 3}} + \ldots$$
$$= 2\sin\left(\frac{\pi}{n}\right) + \frac{1}{2}\sin\left(\frac{\pi}{n}\right)(\omega t_{n,1})^2 \pm \frac{1}{3}\cos\left(\frac{\pi}{n}\right)(\omega t_{n,0})^3 + \ldots$$
$$= 2\sin\left(\frac{\pi}{n}\right) + 2\left(\frac{\omega r}{v}\right)^2\sin^3\left(\frac{\pi}{n}\right) \pm \frac{8}{3}\left(\frac{\omega r}{v}\right)^3\cos\left(\frac{\pi}{n}\right)\sin^3\left(\frac{\pi}{n}\right) + \ldots$$

Where $\omega t_{n,p}$ is ωt_n up to order p on x. At order one: $t_{n,1} = t_{n,0} = 2r/v\ \sin(\pi/n)$. The expression for Δt in equation (6) is now proven.

Appendix B. Relativistic

The calculation to demonstrate equation (9) is analogous to the classical case and the notations are the same, but the relativistic case is more complex and an iterative method is used.

From equation (8):

$$r^2 = \frac{[v\cos\alpha_n t_n + r(1+\beta_D\gamma_D\beta_c\sin\alpha_n)]^2 + (\gamma_D v\sin\alpha_n + c\beta_D)^2 t_n^2}{(1+\beta_D\gamma_D\beta_c\sin\alpha_n)^2}$$

$$\text{and}\quad \tan(\pm 2\pi/n + \omega t_n) = \frac{(\gamma_D v\sin\alpha_n + c\beta_D)t_n}{v\cos\alpha_n t_n + r(1+\beta_D\gamma_D\beta_c\sin\alpha_n)}$$

The method is the same:

$$\begin{cases} \dfrac{v\cos\alpha_n t_n}{r} = (1+\beta_D\gamma_D\beta_c\sin\alpha_n)\left(\dfrac{1}{\sqrt{1+\tan^2\theta'_n}} - 1\right) & \text{if}\quad n>4\quad\text{then}\quad x'_n \geqslant 0 \\ \dfrac{v\sin\alpha_n t_n}{r} = \dfrac{1}{\gamma_D}\left(\pm\dfrac{1+\beta_D\gamma_D\beta_c\sin\alpha_n}{\sqrt{1+1/\tan^2\theta'_n}} - \omega t_n\right) & \text{if}\quad \text{counterclockwise}\quad y'_n \geqslant 0\quad\text{else}\quad y'_n < 0 \end{cases}$$

The orders are now considered. For example, $t_{n,p}$ is t_n up to order p on ϵ:

$$\omega t_{n,p+1} = \epsilon(1+\beta_D\gamma_D\beta_c\sin\alpha_{n,p-1})\times \sqrt{\left[\cos\left(\frac{2\pi}{n}\pm\omega t_{n,p}\right)-1\right]^2 + \frac{1}{{\gamma_D}^2}\left[\pm\sin\left(\frac{2\pi}{n}\pm\omega t_{n,p}\right) - \frac{\omega t_{n,p}}{1+\beta_D\gamma_D\beta_c\sin\alpha_{n,p-1}}\right]^2} \tag{B1}$$

$$\sin\alpha_{n,p} = \epsilon\frac{1+\beta_D\gamma_D\beta_c\sin\alpha_{n,p-1}}{\gamma_D\omega t_{n,p+1}}\left[\pm\sin\left(\frac{2\pi}{n}\pm\omega t_{n,p}\right) - \frac{\omega t_{n,p}}{1+\beta_D\gamma_D\beta_c\sin\alpha_{n,p-1}}\right] \tag{B2}$$

β_D and γ_D are expressed as functions of ϵ and β_c: $\beta_D\gamma_D\beta_c = \epsilon{\beta_c}^2\gamma_D$, $\gamma_D = 1/\sqrt{1-\epsilon^2{\beta_c}^2}$. So ωt_n and $\sin\alpha_n$ can be expanded on ϵ. For the first non-null orders:

$$\omega t_{n,1} = 2\epsilon\sin\frac{\pi}{n} \qquad \text{and} \qquad \sin\alpha_{n,0} = \pm\cos\frac{\pi}{n}$$

Then with equation (B1) and $p=1$, $\omega t_{n,2}$ is obtained, and after with equation (B2) $\sin\alpha_{n,1}$:

$$\omega t_{n,2} = 2\epsilon\sin\frac{\pi}{n} \pm 2\epsilon^2{\beta_c}^2\sin\frac{\pi}{n}\cos\frac{\pi}{n} \qquad \text{and} \qquad \sin\alpha_{n,1} = \pm\cos\frac{\pi}{n} - 2\epsilon\sin^2\frac{\pi}{n}$$

The same equations with $p=2$ are iterated:

$$\omega t_{n,3} = \omega t_{n,2} + \epsilon^3\sin\frac{\pi}{n}\left[2\sin^2\frac{\pi}{n} + {\beta_c}^2\left(1-5\sin^2\frac{\pi}{n}\right)\right]$$

$$\text{and} \qquad \sin\alpha_{n,2} = \sin\alpha_{n,1} \mp \frac{3}{2}\epsilon^2\sin^2\frac{\pi}{n}\cos\frac{\pi}{n}(2+{\beta_c}^2)$$

Then with $p=3$:

$$\omega t_{n,4} = \omega t_{n,3} \pm \epsilon^4\sin\frac{\pi}{n}\cos\frac{\pi}{n}\left[\frac{8}{3}\sin^2\frac{\pi}{n} - 4{\beta_c}^2\sin^2\frac{\pi}{n} - 2{\beta_c}^4\left(2\sin^2\frac{\pi}{n}-1\right)\right]$$

equation (9) is now proved.

ORCID iDs

Mathieu Rouaud https://orcid.org/0000-0002-6728-8278

References

[1] Sagnac G 1913 Sur la preuve de la réalité de l'éther lumineux par l'expérience de l'interférographe tournant *Compt. Rend.* **157** 1410 English: regarding the proof for the existence of a luminiferous ether using a rotating inteferometer experiment.

[2] Rauch H, Treimer W and Bonse U 1974 Test of a single crystal neutron interferometer *Phys. Lett. A* **47** 369–71

[3] Werner S A, Staudenmann J-L and Colella R 1979 Effect of earth's rotation on the quantum mechanical phase of the neutron *Phys. Rev. Lett.* **42** 1103–6

[4] Marton L 1952 Electron Interferometer *Phys. Rev.* **85** 1057

[5] Keith D W, Ekstrom C R, Turchette Q A and Pritchard D E 1991 An interferometer for atoms *Phys. Rev. Lett.* **66** 2693–6

[6] Lenef A, Hammond T D, Smith E T, Chapman M S, Rubenstein R A and Pritchard D E 1997 Rotation sensing with an atom interferometer *Phys. Rev. Lett.* **78** 760

[7] Gustavson T L, Bouyer P and Kasevich M A 1997 Precision rotation measurements with an atom interferometer gyroscope *Phys. Rev. Lett.* **78** 2046–9

[8] Post E J 1967 Sagnac effect *Rev. Mod. Phys.* **39** 475

[9] Rindler W 2006 *Relativity: Special, General, and Cosmological* 2nd edn (Oxford Univ. Press) Synchronization of clocks.

[10] Møller C 1952 *The Theory of Relativity* (Oxford) 1st edn p 222
[11] Pascoli G 2017 The Sagnac effect and its interpretation by Paul Langevin *C.R. Phys.* **18** 563–9
[12] Apostolyuk V 2006 *Theory and Design of Micromechanical Vibratory Gyroscopes* (Springer) ISBN : 978-0-387-24520-1
[13] Rizzi G and Ruggiero M L 2003 A direct kinematical derivation of the relativistic sagnac effect for light or matter beams *Gen. Relativ. Gravit.* **35** 2129–36
[14] Rizzi G and Ruggiero M L (ed) 2003 *Relativity in Rotating Frames: Relativistic Physics in Rotating Reference Frames* vol 135 (Springer Science & Business Media) See on page 37 and 383
[15] Malykin G 2000 The Sagnac effect : correct and incorrect explanations *Phys.-Uspekhi* **43** 1229
[16] Rouaud M 2020 *Special Relativity, A Geometric Approach* 149–55 http://voyagepourproxima.fr/SR.pdf
[17] Landau L and Lifchitz E The classical Theory of Fields *Rotation.*
[18] Einstein A 1917 *Relativity: The Special and General Theory*
[19] Wang R, Zheng Y and Yao A 2004 Generalized sagnac effect *Phys. Rev. Lett.* **93** 143901
[20] Ori A and J E Avron 2016 A Generalized Sagnac-Wang-Fizeau formula *Phys. Rev. A.* **94** 063837
[21] Bongs K, Holynski M, Vovrosh J, Bouyer P, Condon G, Rasel E, Schubert C, Schleich W and Roura A 2019 Taking atom interferometric quantum sensors from the laboratory to real-world applications *Nat. Rev. Phys.* **1** 731–9
[22] Garrido Alzar C L 2019 Compact chip-scale guided cold atom gyrometers for inertial navigation: enabling technologies and design study *AVS Quantum Sci.* **1** 014702
[23] Cronin A D, Schmiedmayer J and Pritchard D E 2009 Optics and interferometry with atoms and molecules *Rev. Mod. Phys.* **81** 1051
[24] Chebotayev V P, Ya B, Dubetsky, Kasantsev A P and Yakovlev V P 1985 Interference of atoms in separated optical fields *J. Opt. Soc. Am. B* **2** 1791
[25] Antoine C and Bordé C J 2003 Quantum theory of atomic clocks and gravito-inertial sensors: an update *J. Opt. B: Quantum Semiclass. Opt.* **5** S199
[26] Anandan J 1981 Sagnac effect in relativistic and nonrelativistic physics *Phys. Rev. D* **24** 338